ACS OMEGA

http://pubs.acs.org/journal/acsodf

Article

Effect of Dielectric Saturation on Ion Activity Coefficients in Ion Exchange Membranes

Akhilesh Paspureddi,* Mukul M. Sharma, and Lynn E. Katz

Cite This: *ACS Omega* 2022, 7, 30823−30834

Read Online

ACCESS | Metrics & More | Article Recommendations | Supporting Information

ABSTRACT: Polymeric ion exchange membranes are used in water purification processes to separate ions from water. The distribution and transport of ionic species through these membranes depend on a variety of factors, including membrane charge density, morphology, chemical structure, and the specific ionic species present in the fluid. The electrical potential distribution between membranes and solutions is typically described using models based on Donnan theory. An extension of the original theory is proposed to account for the nonideal behavior of ions both in the fluid and in the membrane as well to provide a more robust description of interactions of solutes with fixed charge groups on the polymer backbone. In this study, the variation in dielectric permittivity in the membrane medium with electric field strength is taken into account in a model based on Gouy−Chapman double-layer theory to provide a more accurate description of ion activity coefficients in an ion exchange membrane. A semianalytical model is presented that accounts for the variation in dielectric permittivity of water in a charged polymer membrane. A comparison of this model with Manning's counterion condensation model clearly demonstrates that by incorporating changes in water dielectric permittivity with electric field strength, much better agreement with experiments can be obtained over a range of salt concentrations for different ions.

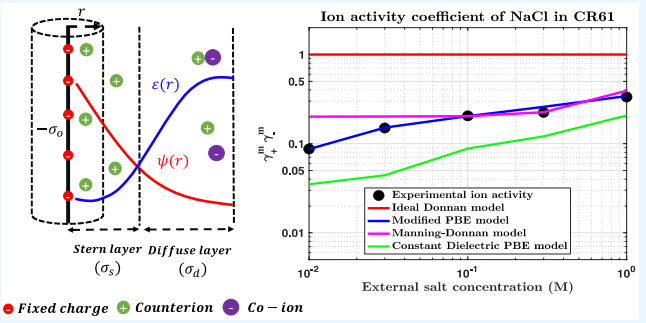

HIGHLIGHTS

- Large electric fields inside an IEM give rise to changes in solution dielectric permittivity.
- A general EDL theory which accounts for changes in dielectric permittivity and in the hydration free energy of ions is presented.
- The modified PBE model is used to model the ion activity coefficients inside an IEM.
- The modified PBE model more closely matches experimental data than does the Manning−Donnan model over a range of salt concentrations.
- The model is quite general and can be applied to any IEM and any ion type.

INTRODUCTION

Ion exchange membranes (IEMs) are polymeric membranes bearing charged functional groups (e.g., sulfonate and quaternary ammonium groups) on the chain backbone.[1,2] IEMs are categorized as cation exchange membranes (CEMs) if they have negative fixed charge groups on the polymer backbone or anion exchange membranes (AEMs) if the fixed charge groups are positively charged. The presence of fixed charge groups requires an electrically equivalent number of counterions to balance the fixed charges, and the fixed charge groups act to exclude mobile ions of the same charge (i.e., co-ions). IEMs can control the transport of ionic species through the membrane based on applied or internally developed electrostatic potentials.[3]

IEMs are used in electrodialysis for water purification applications[4,5] and in fuel cells for energy generation or fuel generation applications.[6] Improving the efficiency of these processes would benefit from an improved fundamental understanding of ion thermodynamics in IEMs.[7] IEMs of practical importance are often highly charged, and ions sorbed into such membranes often exhibit highly nonideal thermodynamic behavior.[1] These nonidealities are often reported in terms of ion activity coefficients.[8] A number of reliable models for ion activity coefficients in aqueous solutions originate from the Debye−Hückel theory of dilute solutions[9] (see review by Robinson and Stokes[10] for more details). However, the literature addressing the thermodynamics of electrolytes in IEMs is not as well-established. Most ion activity models in IEMs typically assume that the dielectric permittivity of the

Received: April 11, 2022
Accepted: August 2, 2022
Published: August 24, 2022

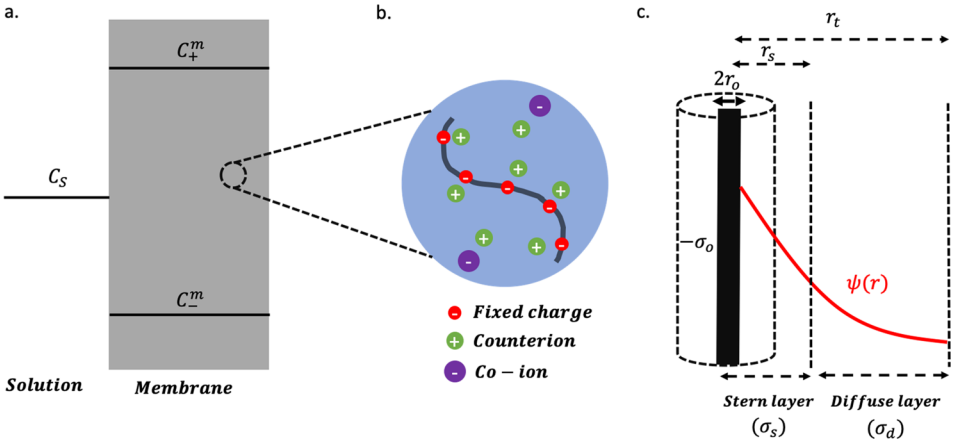

Figure 1. (a) Diagram of a cation exchange membrane equilibrated with salt solution at an external concentration of C_S. The counterion concentration is C_+^m, and co-ion concentration is C_-^m. (b) Diagram of ion distribution around the polymer in an ion exchange membrane. The polymer chain is represented by a solid line. (c) Structure of the double layer around the charged polymer. The charge density at the fixed charge groups is denoted by $-\sigma_0$, the Stern layer charge density is denoted by σ_S, and the diffuse layer charge density is denoted by σ_d. The diameter of the polymer is denoted by $2r_0$. The size of the Stern layer from the center of the polymer is denoted by r_s, and the total double-layer radius from the center of the polymer is denoted by r_t. An example potential profile ($\psi(r)$) around a polymer is shown by the red curve.

solvent medium is constant, which is a reasonable assumption in most instances. However, polymer chemistry and water content have been shown to significantly affect dielectric permittivity.[11] In highly charged IEMs, the electric field in the membrane can be quite large. This can lead to dielectric saturation. Dielectric saturation refers to changes in the dielectric permittivity (i.e., dielectric constant) of the medium due to a high electric field.[11] Dielectric permittivity is often reported to be low in IEMs due, partially, to high electric field strengths in the membrane.[12] The dielectric permittivity affects the Gibbs free energy and, in turn, ion activity coefficients, and hence accurately accounting for dielectric permittivity is important to accurately estimate ion activity coefficients. Hence, changes in dielectric permittivity have been shown to greatly influence ion sorption and ion transport mechanisms in IEMs.[11]

The earliest work on the thermodynamics of IEMs was done by Ostwald,[13] who hypothesized that like charged ions (i.e., co-ions) would be excluded from an IEM. Ostwald's work was extended by Donnan,[14] who studied the ionic equilibria and potential in a charged membrane. However, subsequent research showed that co-ion sorption prediction based on an ideal Donnan equilibrium was poor, especially for low external salt solution concentrations.[15−17] Most recent work that has done a good job of modeling the thermodynamics of IEMs used the Manning−Donnan model.[18] This work employed Manning's counterion condensation theory to account for the nonideal behavior of ions in IEMs and the Pitzer model to account for the nonideal behavior of ions in the external solution.[19] The Manning−Donnan model provides reasonable predictions of ion activity coefficients in IEMs at salt concentrations typical of desalination systems with only one adjustable parameter, which can often be estimated a priori based on the knowledge of the membrane chemical structure and the water uptake. However, in several cases, this model exhibits systematic deviations from experimental data, particularly at low external salt concentrations.[18,20]

In this study we will present a thermodynamic model for ion partitioning and ion activity in IEM using the Poisson−Boltzmann equation (PBE). PBE provides a rational starting point for describing ion distribution around a charged surface immersed in an electrolyte. A key advantage of the PBE is that it can be modified to account for complex descriptions of the electrical double layer surrounding a charged surface and still approach the original description of the interfacial regions set forth by Debye and Hückel for relatively dilute electrolyte solutions.[21] Several researchers have used PBE-based models in the past to describe ion equilibrium around charged surfaces.[22−25] Pintauro et al.[26−28] in a series of papers formulated a PBE-based model to describe equilibrium partitioning of ions into Nafion membranes. However, very high surface potentials (e.g., −1.5 V) and counterion surface concentrations (e.g., 12000 mol/m^3) were shown in this work.[28] In the literature, membrane potential values are often reported to be on the order of ∼100 mV for the polymer−water interface.[29,30] Incorporating a Stern layer[31] into the description of the electrical double layer reduces the very high model predictions of ion concentrations for highly charged IEMs.

The model proposed in this study uses the PBE, modified to include dielectric saturation, ion dehydration, and a Stern layer of condensed ions, to calculate ion concentration profiles in a dense, nonporous charged membrane. The modified PBE model is then used to explain the influence of polymer charge density on dielectric permittivity and demonstrate the effect of a Stern layer on charge distribution within the interfacial region of the membrane. Ion activity coefficients determined using this thermodynamic framework are compared to values obtained from the Manning−Donnan model and experimental data.

MODEL FORMULATION

The dense IEM considered in this work is a commercially available cation exchange membrane, CR-61, from Suez (formerly GE Water). Chemically, it is a cross-linked network prepared by copolymerizing sulfonated styrene and divinylbenzene.[18] CR-61 has a composite structure consisting of ion exchange resin polymerized into a hydrophobic, porous fabric backing that provides mechanical support to the mechanically fragile (i.e., brittle) ion exchange resin.[32] When such a charged membrane is in equilibrium with an electrolyte solution, a

https://doi.org/10.1021/acsomega.2c02258
ACS Omega 2022, 7, 30823−30834

potential difference is established between the membrane and the solution.[16] A cartoon of this equilibrium is shown in Figure 1a. To neutralize the fixed charges inside the membrane, high concentrations of counterions (C_+^m) exist inside a membrane (often greater than in the external solution). This unequal ion distribution creates a potential difference at the membrane−solution interface. The difference between the membrane potential and the solution potential is the Donnan potential. However, because the charges in an IEM are dispersed in a finite volume, there should be a continuous change in potential across the membrane−solution interface rather than a discontinuous Donnan type potential.[33] To account for the continuous potential, we explicitly model the polymer−water interface that exists inside a membrane. A cartoon depicting counterion condensation around the polymer and a corresponding description of the interfacial region of an IEM is shown in Figure 1b,c, respectively. Electrostatic interactions within the membrane were modeled by treating the polymer chain inside the membrane as an infinitely long cylindrical rod with a constant fixed charge, as shown in Figure 1c. The complete picture of the double layer modeled in this work is shown in Figure S1 in the Supporting Information. The electrolyte confined between two infinitely long charged polymer rods is modeled using Stern−Gouy−Chapman theory. This system is in equilibrium with the external salt concentration (C_S), and solving the Poisson−Boltzmann equation in the domain gives us the ion distribution adjacent to the polymer having a constant fixed density of $-\sigma_0$, as shown in Figure 1c. Any local polymer chain−polymer chain interactions are assumed to be screened by the condensed ions in the Stern layer. Additional assumptions are as follows.

i. The ions are point charges.
ii. The bounding surfaces are ideally polarizable.
iii. The fixed charge density is uniform.
iv. Water is a dielectric continuum whose dielectric permittivity changes as a function of local electric field strength.
v. The thickness of the Stern layer depends on the Stokes radius of the solute ions.[34,35]
vi. The fixed charge density is assumed to be constant (i.e., any changes in membrane swelling with changes in ion concentration are neglected).[36]

MODIFIED PBE FOR A SOLVENT WITH VARIABLE DIELECTRIC PERMITTIVITY

The starting point for this study was inspired by a previous application of a modified Poisson−Boltzmann equation to membrane materials by Basu and Sharma.[37] For a charged surface immersed in a dielectric medium containing ions, the electrical potential distribution in the radial direction, normal to the surface, is given by the Poisson equation

$$\left\{\frac{1}{r}\frac{\mathrm{d}}{\mathrm{d}r}\left(r\varepsilon\frac{\mathrm{d}\psi}{\mathrm{d}r}\right) = -\frac{\rho}{\varepsilon_0}\right\} \tag{1}$$

where ε and ε_0 are the dielectric permittivities of the medium and free space, respectively, ψ is the potential in V, r is the radial distance, and ρ is the charge density given by

$$\rho = e\sum_{N}^{i=1} z_i c_i^m(r) \tag{2}$$

where e is the charge of an electron, z_i is the valence of the ith ion, and $c_i^m(r)$ is the concentration of the ith ion in moles of ions per liter. To model ρ appropriately, all forces acting on ions in the free volume around the charged polymer must be considered, and this is typically done by considering the potential from the surface. Ion concentrations are generally assumed to follow a Boltzmann distribution with distance away from the charged polymer into a medium of constant dielectric permittivity[38,39]

$$c_i^m(r) = c_i^b \exp\left[-\left(\frac{ez_i}{kT}\right)\psi(r)\right] \tag{3}$$

where c_i^b is the bulk ion concentration, k is the Boltzmann constant, and T is the absolute temperature. The bulk ion concentration is used as the proportionality constant in eq 3 because the polymer in the IEM is in equilibrium with the external salt solution. We assume that this external salt concentration affects the concentration of ions confined inside the IEM.

However, if the ions reside in a medium with variable dielectric permittivity, an additional electrostatic free energy contribution is associated with their movement from a medium of high to low dielectric permittivity.[40,41] This contribution arises from the fact that the water molecules in this low dielectric region are highly ordered, and for ions to exist in hydrated form, they should align these water molecules toward the ion center rather than toward the external electric field. This change in the free energy, ΔG_i, is given by the Born equation[40]

$$\Delta G_i = \frac{z_i^2 e^2}{8\pi\varepsilon_0 r_i}\left(\frac{1}{\varepsilon(r)} - \frac{1}{\varepsilon_b}\right) \tag{4}$$

$$H_i = \frac{z_i^2 e^2}{8\pi\varepsilon_0 r_i} \tag{5}$$

where r_i is the radius of the ith ion and $\varepsilon(r)$ and ε_b are the dielectric permittivities of the medium at a distance r and in the bulk, respectively. The leading term in eq 4 can be evaluated for most ions and is denoted as H_i, the hydration constant for the ith ion. Experimental values for H_i are recorded in Table 1.

Table 1. Hydration Constant, H_i, Values for Ions at 25 °C[37]

ion	H_i (kJ/mol)
Li^+	531.7
Na^+	430.9
K^+	356.0
Cs^+	301.6
Cl^-	292.8
Br^-	266.9
H^+	1096.2

Incorporating the above equations into a modified Boltzmann distribution (to account for the variable dielectric permittivity), we obtain an expression for the distribution of ions, $c_i^m(r)$, in the double layer near the charged polymer backbone:

$$c_i^m(r) = c_i^b \exp\left[-\left(\frac{ez_i}{kT}\right)\psi(r) - \left(\frac{H_i}{kT}\right)\left(\frac{1}{\varepsilon(r)} - \frac{1}{\varepsilon_b}\right)\right] \tag{6}$$

https://doi.org/10.1021/acsomega.2c02258
ACS Omega 2022, 7, 30823−30834

The first term inside the exponential corresponds to the electrostatic energy, and the second term is related to the hydration energy of the ions. Equeation 6 reduces to the classic Boltzmann distribution if the dielectric permittivity is constant.[37]

Using the definition of electric field, $E = -\mathrm{d}\psi/\mathrm{d}r$, in eq 1 gives

$$\frac{\mathrm{d}^2\psi(r)}{\mathrm{d}r^2} = -\frac{\rho}{\varepsilon_0\left(\varepsilon + E\frac{\mathrm{d}\varepsilon}{\mathrm{d}E}\right)} + \frac{\varepsilon E}{r\left(\varepsilon + E\left(\frac{\mathrm{d}\varepsilon}{\mathrm{d}E}\right)\right)} \tag{7}$$

Substituting eqs 2 and 6 into eq 7 and rearranging yields

$$\frac{\mathrm{d}^2\psi(r)}{\mathrm{d}r^2} = -\frac{e\sum_{i=1}^{N} c_i^{\mathrm{b}} z_i \exp\left[-\left(\frac{ez_i}{kT}\right)\psi(r) - \left(\frac{H_i}{kT}\right)\left(\frac{1}{\varepsilon(r)} - \frac{1}{\varepsilon_{\mathrm{b}}}\right)\right]}{\varepsilon_0\left(\varepsilon(r) + E(r)\left(\frac{\mathrm{d}\varepsilon(r)}{\mathrm{d}E(r)}\right)\right)} + \frac{\varepsilon(r)E(r)}{r\left(\varepsilon(r) + E(r)\left(\frac{\mathrm{d}\varepsilon(r)}{\mathrm{d}E(r)}\right)\right)} \tag{8}$$

where $\varepsilon(r)$ can be described as a function of electric field strength as given in Basu and Sharma (1994)[37]

$$\varepsilon(r) = \eta^2 + (\varepsilon_{\mathrm{b}} - \eta^2)\left(\frac{3}{\beta E(r)}\right)\left[\coth(\beta E(r)) - \frac{1}{\beta E(r)}\right] \tag{9}$$

$$\beta = \frac{5\mu}{2kT}(\eta^2 + 2) \tag{10}$$

for $E(r)$ greater than 2.0×10^7 V/m. Here, β is 1.41×10^{-8} m/V, η (=1.33) is the refractive index of water, and μ ($=6.17 \times 10^{-30}$ cm) is the dipole moment of a water molecule.

For $E(r)$ less than 2.0×10^7 V/m, the permittivity is as presented by Grahame et al.[41]

$$\varepsilon(r) = \frac{\varepsilon_{\mathrm{b}}}{E(\sqrt{q})}\tan^{-1}(E(\sqrt{q})) \tag{11}$$

where $q = 1.2 \times 10^{-13}$ cm^2/V^2. Significant changes in dielectric constant occur at electric field strengths greater than about 10^8 V/m. In most highly charged ion exchange membranes, field strengths in excess of this value will likely be obtained.[33]

NUMERICAL COMPUTATION

Equation 1 is a second-order stiff differential equation, which was converted into a system of two first-order differential equations yielding a boundary value problem. The symmetry surface between adjacent polymers is shown in Figure S1 in the Supporting Information. Because CR61 is a highly charged IEM, we would observe overlapping double layers as shown in Figure S1. Due to symmetry, this modified PBE is solved for half of the free volume between polymers inside the IEM. The symmetry condition as well as the charge balance can be written as

$$\left(\frac{\mathrm{d}\psi}{\mathrm{d}r}\right)_{r=r_{\mathrm{t}}} = 0 \quad \psi_{r=r_{\mathrm{t}}} = \psi_{\mathrm{m}} \tag{12}$$

and

$$-\frac{1}{r_{\mathrm{s}}}\int_{r=r_{\mathrm{s}}}^{r=r_{\mathrm{t}}} \rho(\psi, \varepsilon(r))r\ \mathrm{d}r = \sigma_{\mathrm{d}} \tag{13}$$

where r_{t} and r_{s} are respectively the total radius of free volume and radius up to the Stern layer location, ψ_{m} is the potential value when $r = r_{\mathrm{t}}$, and σ_{d} is the total charge density in the diffuse layer of the free volume. We can also write

$$\sigma_0 = \sigma_{\mathrm{s}} + \sigma_{\mathrm{d}} \tag{14}$$

where σ_0 and σ_s are the charge densities on the polymer surface and in the Stern layer, respectively. The thickness of the Stern layer is taken to be constant for a given counterion.[35] The thickness of the Stern layer is an adjustable parameter, and it is chosen based on the Stokes diameter of the ions. While researchers in the past (such as Brown et al.[35]) have provided higher Stern layer thicknesses, since IEMs have higher charge density the condensed ions are considered to be dehydrated. Due to high electric field strengths close to the polymer charge groups, condensed ions in IEMs have been reported to be dehydrated and hence have a smaller size in the Stern layer (Table 2).[42] Further study is required to experimentally validate Stern layer thicknesses for different counterions in IEMs.

Table 2. Stern Layer Thickness for Different Counterions in This Study

ion	x_{s} (Å)
Li^+	4
Na^+	3
K^+	2

With these boundary conditions, the PBE was solved using a generalized Runge−Kutta method.[43] An iterative procedure was used by first choosing ψ_{m} and then solving the modified PBE equation to get σ_{d}, used as the boundary condition.

The modified-PBE with variable dielectric permittivity has multiple solutions, and it is easy to show by simply integrating eq 1 from r_{o} to r_{t}, where r_{o} is the radius of the polymer and r_{t} is the distance to the center line between polymer surfaces.

$$\left(\frac{\mathrm{d}\psi}{\mathrm{d}r}\right)_{r=r_{\mathrm{o}}} = \frac{1}{\varepsilon_0\varepsilon r_{\mathrm{o}}}\int_{r_{\mathrm{o}}}^{r_{\mathrm{t}}} \rho r\ \mathrm{d}r = \frac{-\sigma_{\mathrm{s}}}{\varepsilon_0\varepsilon} \tag{15}$$

By plotting σ_{s} and $E(r)\varepsilon_0\varepsilon$ against $E(r)$, it can be shown that there are multiple solutions to eq 8 in the case of variable dielectric permittivity but only one solution for a constant dielectric permittivity. This has been shown in our previous work.[44] It has no implications for the model results because there is only one physically reasonable solution.

ION CONCENTRATION AND ACTIVITY

Concentration. Counterion and co-ion concentrations in the double layer are computed by averaging over the potential and electric field in the double layer (shown in eq 8). The overall concentrations for counterion and co-ion for a negatively charged IEM are computed as averages of the charge stored in the Stern and diffuse layers of the electrical double layer as shown in eqs 16 and 17, respectively.

$$\bar{C}_+^{\mathrm{m}} = \frac{\frac{-\sigma_s r_p}{F} \times 10^7 + \int_{r_{\mathrm{s}}}^{r_{\mathrm{t}}} C_+^{\mathrm{m}}(r) r\ \mathrm{d}r}{\int_{r_{\mathrm{o}}}^{r_{\mathrm{t}}} r\ \mathrm{d}r} \tag{16}$$

https://doi.org/10.1021/acsomega.2c02258
ACS Omega 2022, 7, 30823−30834

$$\bar{C}_-^{\,m} = \frac{\int_{r_s}^{r_t} C_-^{m}(r) r \, dr}{\int_{r_o}^{r_t} r \, dr} \tag{17}$$

where $\bar{C}_+^{m}$ and $\bar{C}_-^{m}$ are the overall concentrations for the counterion and co-ion for a negatively charged IEM, respectively. r_o is the polymer radius in Å, r_s is the Stern layer radius in Å, r_t is the radius of the entire double layer in Å, σ_s is the Stern layer charge density in C/m^2, and F is Faraday's constant. The complete set of parameters needed to compute concentrations shown in eqs 16 and 17 is presented in Table S1 in the Supporting Information.

Ion Activity. The condition for thermodynamic equilibrium is derived using the electrochemical potential $\bar{\mu}_i^{m}$ as given by Guggenheim[45]

$$\bar{\mu}_i^{j} = \bar{\mu}_i^{j0} + RT \ln(\gamma_i^{j} C_i^{j}) + z_i F \psi^{j} + \bar{V}_i^{j}(P^{j} - P_0) \tag{18}$$

where $\bar{\mu}_i^{j0}$, γ_i^{j}, C_i^{j}, and $\bar{V}_i^{j}$ are the standard state chemical potential, activity coefficient, concentration, and partial molar volume of ion i in phase j, respectively. T is the absolute temperature, R is the universal gas constant, z_i is the valency of ion i, F is Faraday's constant, ψ^{j} is the electrostatic potential for phase j, P^{j} is the hydrostatic pressure in phase j, and P_0 is the reference pressure. At equilibrium, the electrochemical potential of each diffusing species is equal in the two phases:

$$\bar{\mu}_i^{m} = \bar{\mu}_i^{s} \tag{19}$$

where $\bar{\mu}_i^{m}$ and $\bar{\mu}_i^{s}$ are the electrochemical potentials in the membrane and solution phases for species i, respectively. Applying the condition in eq 18 to both counterions and co-ions, we obtain eqs 20 and 21.

$$RT \ln\left(\frac{\gamma_+^{s} C_+^{s}}{\gamma_+^{m} C_+^{m}}\right) = F(\psi^{m} - \psi^{s}) + \bar{V}_+^{m}(P^{m} - P^{s}) \tag{20}$$

$$RT \ln\left(\frac{\gamma_-^{s} C_-^{s}}{\gamma_-^{m} C_-^{m}}\right) = -F(\psi^{m} - \psi^{s}) + \bar{V}_-^{m}(P^{m} - P^{s}) \tag{21}$$

The partial molar volume is assumed to be the same in both phases and to be independent of pressure. The high molar volume of salts, which increases almost linearly with the square root of the ionic strength, makes the partial molar term smaller than the electrostatic and activity terms in eq 20 and 21.[46] Combining eq 21 and 22 and neglecting molar volume terms, the product of ion activity coefficients, $\gamma_+^{m}\gamma_-^{m}$, in an IEM is given by

$$\gamma_+^{m}\gamma_-^{m} = \frac{(\gamma_\pm^{S})^2 (C_S)^2}{C_+^{m} C_-^{m}} \tag{22}$$

The ratio of ion activity coefficients in solution to those in the membrane is given by

$$\Gamma = \frac{(\gamma_\pm^{S})^2}{\gamma_+^{m}\gamma_-^{m}} \tag{23}$$

where $\gamma_\pm^{S}$ and C_S are the mean ion activity and bulk salt concentration, respectively, in the external electrolyte solution. Ion activity coefficients in bulk solution have been widely reported in the literature.[47−50] Pitzer's model is used to estimate bulk ion activity in our work.[48] Ion activity coefficients from the modified-PBE model come from using concentration estimates from eqs 16 and eq 17 in eq 22.

Manning's Model. In Manning's model, a polymer chain is modeled as an infinitely long line charge with fixed charge groups equally spaced, a distance b apart from each other, along the chain.[19] Manning's theory has one parameter, ξ, which is the ratio of two length scales

$$\xi = \frac{e^2}{4\pi\varepsilon_0\varepsilon kTb} = \frac{\lambda_B}{b} \tag{24}$$

where λ_B is the Bjerrum length and b is the distance between fixed charges. For a highly charged membrane, b is quite small, and values of ξ greater than 1 are expected. Within Manning's framework, the equation for ion activity coefficients in the membrane is given by

$$\gamma_+^{m}\gamma_-^{m} = \left(\frac{\frac{n_e}{n_s\xi} + 1}{\frac{n_e}{n_s} + 1}\right) \exp\left(\frac{-\frac{n_e}{n_s}}{\frac{n_e}{n_s} + 2\xi}\right) = \left(\frac{\frac{X}{\xi} + 1}{X + 1}\right) \exp\left(\frac{-X}{X + 2\xi}\right) \tag{25}$$

where n_e and n_s are the concentrations of fixed charges and co-ions, respectively, in the membrane phase (in units of mols per unit volume of sorbed water) and $X = n_e/n_s$. When eq 25 is combined with the charge balance given below in eq 26 for the membrane phase, the membrane ion concentration and activity coefficients can be calculated via Manning's model.

$$n_e = n_s + n_c \tag{26}$$

where n_c is the concentration of counterions in the membrane phase (in units of moles per unit volume of sorbed water).

RESULTS AND DISCUSSION

The results from this work are presented in two sections. In the first section, the modified PBE model was used to compute the ion concentrations and dielectric permittivity adjacent to the charged polymer as a function of surface charge density. The effect of dielectric saturation on counterion concentration profiles is illustrated by changing the surface charge density on the polymer surface. The need for inclusion of a Stern layer in the model is demonstrated by comparing calculated potentials to expected values.

In the second part of the work the model is used to describe the ion sorption isotherm of a CR61 membrane, which is a commercial cation exchange membrane whose structure and properties are described in more detail elsewhere.[18] Two model fitting parameters, σ_0 and σ_s, were varied to achieve the best fit between the model and the experimental data. The model was fit to the experimental data by choosing a value of membrane surface charge density, σ_0, and by varying the Stern layer charge density, σ_s, to obtain the best agreement between the experimental counterion and co-ion sorption data and the calculated values from the model. The value of σ_0 is fixed (for all cases), and the value of σ_s is chosen at a given external salt concentration. The value of the diffuse layer charge density, σ_d, is computed from eq 13. By solving the modified PBE in the diffuse layer, we obtain the concentration profiles for both counterions and co-ions. Counterion concentration in the Stern layer is calculated using the value σ_s and Stern layer radius, r_s, as shown in eq 16. The Stern layer radius, r_s, was fixed based on the literature values of Stokes ionic diameters.[34,35] The sum of the Stern layer thickness, $r_s - r_o$,

https://doi.org/10.1021/acsomega.2c02258
ACS Omega 2022, 7, 30823−30834

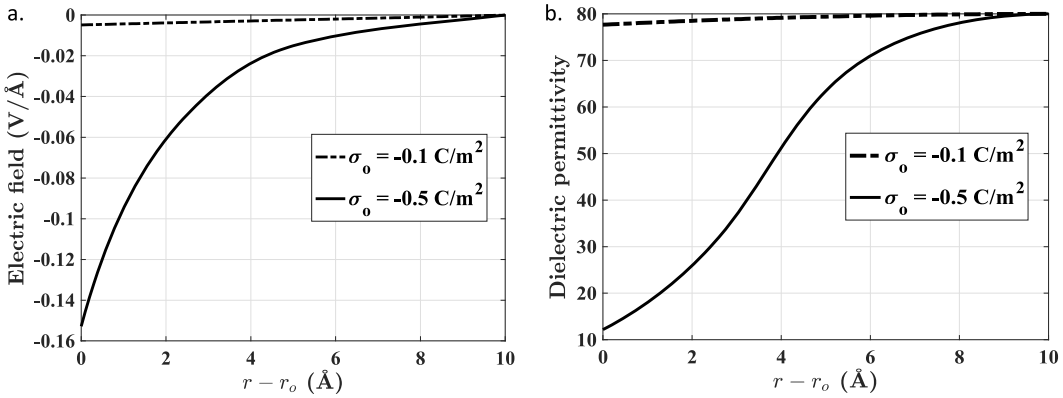

Figure 2. (a) Electric field strength as a function of distance from the polymer for $\sigma_o = -0.1$ C/m^2 (dashed line) and $\sigma_o = -0.5$ C/m^2 (solid line) at an external salt concentration of 0.01 M NaCl, where σ_o is the surface charge density of the polymer. (b) Dielectric permittivity as a function of distance from the polymer for $\sigma_o = -0.1$ C/m^2 (dashed line) and $\sigma_o = -0.5$ C/m^2 (solid line) at an external salt concentration of 0.01 M NaCl. The *X* axis is the distance from the polymer surface, where r_o is the polymer radius.

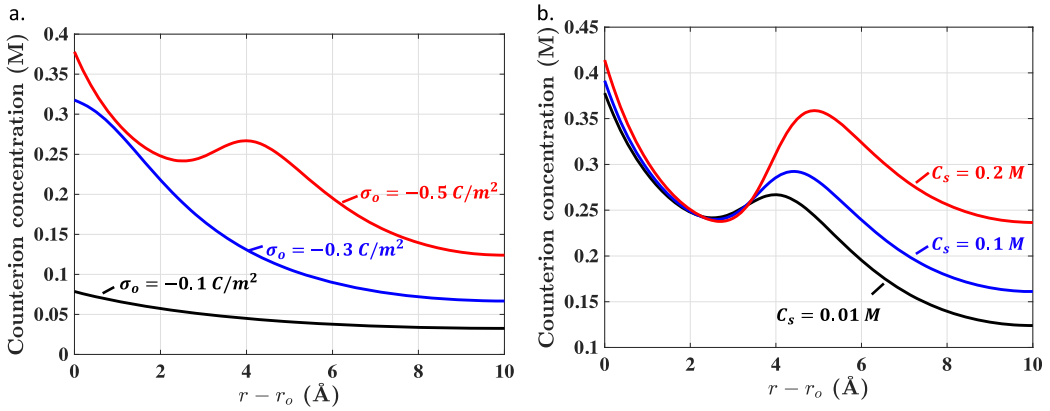

Figure 3. (a) Counterion concentration profile in the EDL for three different surface charge densities at an external salt concentration of 0.01 M NaCl. (b) Counterion concentration profile in the EDL for three different external concentrations for a surface charge density of −0.5 C/m^2, where σ_o is the surface charge density of the polymer and C_S is the external salt (NaCl) concentration. The *X* axis is the distance from the polymer surface, where r_o is the polymer radius.

and the diffuse layer thickness, $r_t - r_s$, was set equal to 10 Å in all cases. Double-layer thickness is an adjustable parameter, and we have used the values based on previous work on charged membranes.[26,37] The radius of the polymer, r_o, is fixed at 5 Å in this work. The radius of the polymer is an adjustable value, and Figure S2 in the Supporting Information shows how its value affects the charge density needed to model ion concentrations in CR61. To achieve a good fit of the model to the experimental ion sorption values across a range of ionic strengths (i.e., external salt concentrations), it is important to consider both the presence of a Stern layer near the charged groups on the polymer chains and to account for dielectric saturation in the solution adjacent to the charged groups. As shown in Figure Figure S3b in the Supporting Information, if one applies the model without a Stern layer to highly charged systems such as the IEM considered here, unrealistically high counterion concentrations (higher than a close packing of dehydrated ions would allow) are observed adjacent to the membrane surface. The effect of neglecting dielectric saturation (i.e., using the PBE model with a constant dielectric permittivity) is shown in Figure 7 and the discussion that follows. The external ion concentration was varied within the range of the experimental results (from 0.01 to 1 M) as described by Kamcev et al.[18]

Effect of Surface Charge Density and Dielectric Saturation on Counterion Concentration Profile. In this section we show the effect of surface charge density on electric field strength, dielectric saturation, and counterion concentration with no Stern layer (i.e., $\sigma_s = 0$). We varied the values of polymer charge density from −0.1 to −0.5 C/m^2. This range of charge densities is consistent with literature values for moderate[37] to highly charged materials.[26−28] Figure 2a shows the electric field strength in an electrolyte solution near a charged surface. As shown in Figure 2b, at high charge density (i.e., −0.5 C/m^2) the dielectric permittivity decreases closer to the surface (i.e., in the region of higher electric field strength). However, in Figure 2b, where a lower surface charge density (i.e., −0.1 C/m^2) is considered, the decrease in dielectric permittivity across the electrical double layer is significantly smaller. Reorientation of water molecules in a strong electric field creates a polarized field of oriented dipoles that reduces the dielectric permittivity,[51] and hence to model the environment around highly charged polymers we need to account for dielectric saturation. In this study, we use the dielectric saturation expression developed by Booth et al.[52] (as shown in eq 9) to account for interactions between the water dipole moment and the electric field generated by a fixed charge on a polymer chain in a membrane. While more simplistic than the theory set forth by Debye,[53] it has been

https://doi.org/10.1021/acsomega.2c02258
ACS Omega 2022, 7, 30823−30834

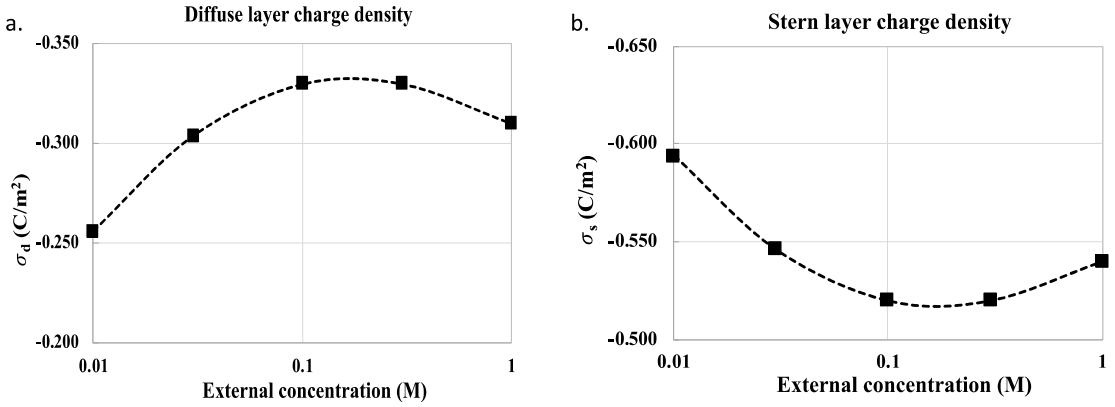

Figure 4. (a) Diffuse layer charge density as a function of external salt concentration for CR61 in NaCl solution. (b) Stern layer charge density as a function of external salt concentration for CR61 in NaCl solution, where σ_d is the charge density in the diffuse layer and σ_s is the charge density in the Stern layer around the polymer. The dashed lines are drawn to guide the eye. The polymer surface charge density (σ_o) used in this work is -0.85 C/m^2.

shown to better predict the dielectric permittivity of strongly polar molecules such as water.[52]

In Figure 3, we present the effect of surface charge density and salt concentration on counterion concentration distribution. Figure 3a shows the effect of surface charge density on counterion concentration profiles. The case with $\sigma_o = -0.1$ C/m^2 corresponds to a relatively low electric field strength, and the water dielectric permittivity remains close to that of bulk water. This leads to a Gouy−Chapman type exponential decay in concentration as a function of distance from the surface, as seen in Figure 3a. However, with a higher surface charge density ($\sigma_o = -0.5$ C/m^2), a peak is evident in the concentration profile. This peak in concentration is evidence of two competing forces. When the hydration energy is accounted for in the Poisson−Boltzmann equation (as shown in eq 6), the ion concentrations show a clear maximum with distance from the charged polymer interface, as shown in Figure 3. This maximum is ascribed to two competing effects: (1) electrostatic attraction of the counterions toward the charged groups on the polymer backbone, resulting in a higher concentration of counterions near the polymer, and (2) ion hydration energy that favors movement of the counterions from regions of high electric field strength or low dielectric permittivity to regions of low electric field (i.e., high dielectric constant). In this case, counterions must overcome an additional hydration energy barrier to move into the region of low dielectric permittivity (i.e., near the fixed charge groups on the polymer backbone). In contrast, Figure 3b shows that the bulk solution ion concentration has little effect on the location of the peak but the value of the peak in the concentration increases with bulk solution ion concentration. The center line counterion concentration is not equal to the external salt concentration because the electrostatic potential at the center line, equidistant between two polymer interfaces, is nonzero.

Application of Modified PBE Model to Ion Exchange Membrane's Ion Sorption Data. In this section, we consider both the Stern layer (with charge density σ_s) and diffuse layer (with charge density σ_d) to model IEMs with higher surface charge density than the values used in the last section. The effect of high surface charge on ion distribution and the need for a Stern layer is justified in Figure S3 in the Supporting Information. We used experimental results for equilibrium uptake of NaCl, LiCl, and KCl in a cation exchange membrane from recent publications.[18,54] The charge density of an ion exchange membrane is related to the ion exchange capacity (IEC) and water uptake of the membrane. CR61 has a reported IEC of 2.2 mequiv/g (dry polymer) and a charge density of 3.21 mol of fixed charge groups per liter of sorbed water (in dilute solutions of NaCl).[18] Under typical working pH conditions, sulfonyl groups are expected to be completely dissociated; thus, the surface charge density is assumed to be a constant for the entire concentration range (0.01−1 M). The surface charge density value (σ_0) for CR61 used in this work is -0.85 C/m^2. This value of charge density is in the range of values used to model IEMs in the past.[26] It is one of the fitting parameters in our model.

To fit ion activity coefficients over a range of salt concentrations, the charge density in the Stern layer is varied. As the solution bulk ion concentration increases, the concentration of ions in the diffuse double layer increases, and the electric field strength increases. An increasingly large percentage of the charge is stored in the diffuse layer due to dielectric saturation. At lower external salt concentration, ions have lower electrostatic energy, and hence, cannot easily cross the energy barrier associated with dielectric saturation close to the polymer. However, at higher ionic strength, the electric field strength becomes large enough in the diffuse layer to allow ions to enter the Stern layer (the electrostatic energy of the ions increases). Beyond this bulk ion concentration, the charge stored in the diffuse layer decreases, and more ions are forced to reside in the Stern layer, as illustrated in Figure 4.

This effect is made obvious if we consider eq 6. The increase in diffuse layer charge density with increasing external concentration continues until the electrostatic energy (first term in the exponential of eq 6) of the ions is comparable to the ion hydration energy (second term in the exponential of eq 6). At this threshold external concentration, counterions can more readily access the low dielectric permittivity region near the fixed charge groups, causing σ_d to decrease. Similarly, as shown in Figure 4b, the Stern layer charge density has a minimum that is set by the same competing forces of electrostatic energy and ion hydration energy.

By using the charge density values above, the electrical potential profiles in the diffuse layer around the polymer−water interface are shown in Figure 5. Ohshima et al.[33] has presented a comprehensive study comparing the classical Donnan discontinuous potential to a more continuous surface

https://doi.org/10.1021/acsomega.2c02258
ACS Omega 2022, 7, 30823−30834

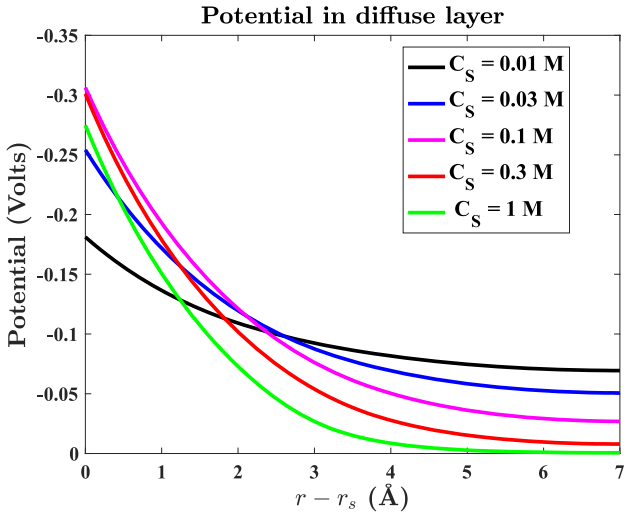

Figure 5. Electrostatic potential profiles in the diffuse layer at different external salt concentrations. C_s is the external salt concentration, and the thickness of the Stern layer is 3 Å for NaCl. The *X* axis is the distance from the Stern layer, where r_s is the size of the Stern layer from the center of the polymer.

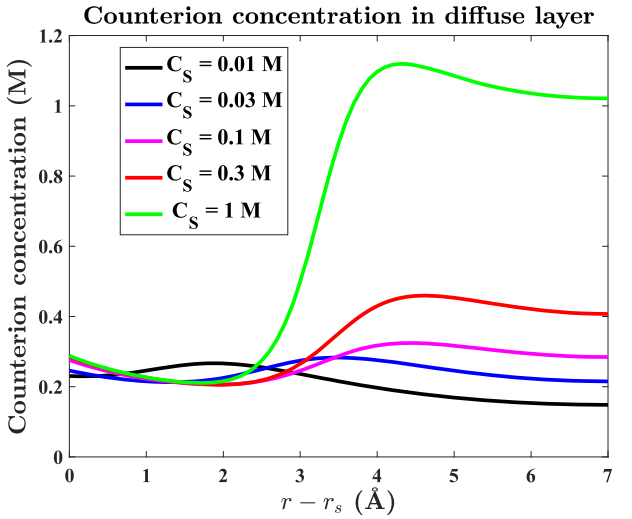

Figure 6. Counterion concentration profiles in the diffuse layer at different external salt concentrations. C_s is the external salt concentration, and the thickness of the Stern layer is 3 Å for NaCl. The *X* axis is the distance from the Stern layer, where r_s is the size of Stern layer from the center of the polymer.

potential.[55] Our current approach in this work is similar to the latter, where we assume that the membrane fixed charges are uniformly distributed, and the PBE is solved to obtain a potential gradient inside the membrane next to the polymer–water interface. This potential difference controls the ion distribution inside the membrane and also facilitates exclusion of co-ions from the membrane.

The potential far from the polymer–water interface (i.e., r = 7 Å) decreases with increasing external salt concentration, consistent with Gouy–Chapman theory. The Stern layer potential (potential at r = 0 Å in the above figure) has a similar trend with σ_s, increasing with increasing counterion concentration in the Stern layer. The center line potential values are less than 100 mV for all external salt concentrations. These values are consistent with ζ potentials reported in the literature for charged membranes.[56] These potential values suggest that our choice of parameters is within the range of measured values.

The dielectric saturation in the diffuse layer for the above potential in Figure 5 is shown in Figure S4 in the Supporting Information. For the potential and dielectric permittivity presented above, the counterion concentration profiles in the diffuse layer are presented in Figure 6. The hydration layer thickness is the distance from the polymer surface to the peak of the concentration profile. Hydration layer thickness is related to the charge density in the diffuse layer; with increasing external concentration, the counterions are excluded from the low dielectric region as shown in Figure 4. As shown in Figure 6, the hydration layer thickness first increases and then decreases as the external salt concentration increases. The reduction in the Stern layer charge causes the region of influence from the fixed charge in the free volume to increase. As discussed earlier, above a certain external concentration (>0.3 M) when the ions have enough electrostatic energy to overcome the hydration energy, the hydration layer thickness decreases.

To elucidate the importance of dielectric saturation on ion concentration and activity coefficients, the results obtained from the modified-PBE are also compared with results using a constant dielectric permittivity PBE model, Manning–Donnan theory, and ideal Donnan theory (Γ = 1). Pitzer's model was used to calculate the mean salt ion activity coefficient in the external solution for all models.[49] In Figure 7, counterion and co-ion concentrations calculated via the modified-PBE model with variable dielectric permittivity are compared to the experimental results from Kamcev et al.,[18] the modified-PBE with an assumption of constant dielectric permittivity, and the Manning–Donnan model. Model concentration values are presented in units of moles of ions per liter to compare directly with experimental data. Not surprisingly, the constant dielectric permittivity model overpredicts co-ion concentration because the hydration energy barrier is zero when the dielectric is the same as that of bulk water from eq 6. Therefore, counterion interactions with the fixed charge are overpredicted and co-ion exclusion from the membrane is underpredicted. Similar issues with co-ion concentration predictions were observed by Delville et al. in using a PBE-based model to describe simple salt activity in the presence of polyelectrolytes.[57] Ideal Donnan theory overpredicts co-ion exclusion, as shown in Figure 7b. This discrepancy is higher at lower external salt concentrations, since differences in ion activity coefficients in the membrane and in solution are neglected, forcing Γ = 1 in the ideal Donnan model. The concentrations of both Na^+ and Cl^- are predicted quite well with the variable dielectric permittivity modified-PBE model. The concentrations presented here are used to predict the ion activity coefficients using eq 22 and are presented in Figure 8.

The experimental ion activity coefficients for NaCl in CR61 were taken from the experimentally determined values of Kamcev et al.[18] In the Manning–Donnan model,[58] ξ = 1.83 is used to calculate mean ion activity coefficients using eq 25. The recently developed Manning–Donnan model is quite simple and predicts experimental ion activity data reasonably well without any fitting parameters.[58] One of the main drawbacks of the Manning–Donnan model, shown in Figure 8, is that it does not match experimental data at dilute external salt concentrations in this particular IEM. This discrepancy is currently believed to occur because it was developed as a

https://doi.org/10.1021/acsomega.2c02258
ACS Omega 2022, 7, 30823–30834

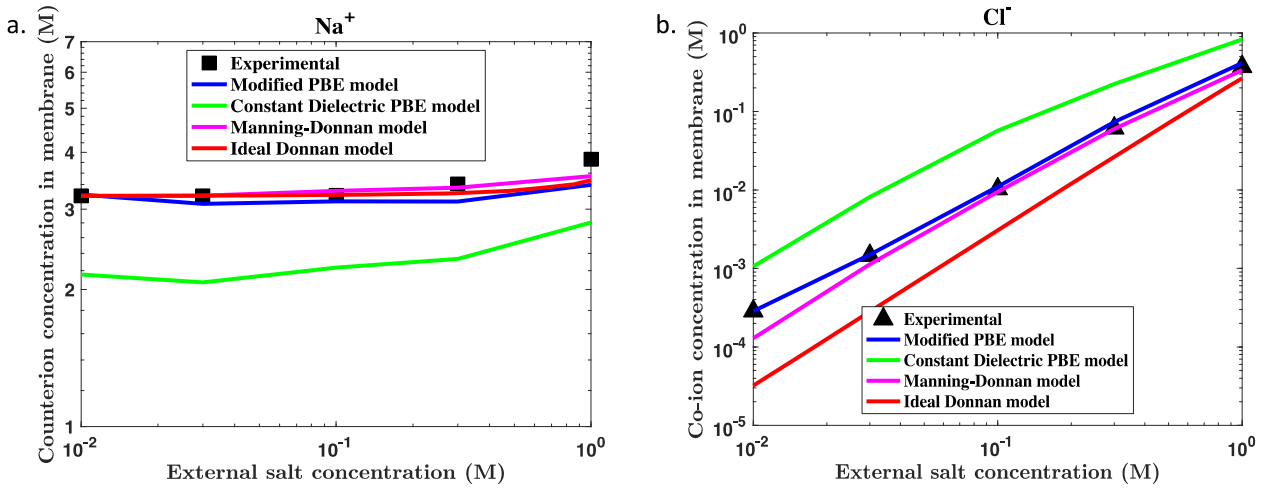

Figure 7. (a) Comparison of counterion (Na^+) concentration for experimental, modified-PBE model, constant fielectric PBE model, Manning–Donnan model, and ideal Donnan model. Experimental results for Na^+ are denoted by ■. (b) Comparison of co-ion (Cl^-) concentration for experimental, modified-PBE model, constant dielectric PBE model, Manning–Donnan model, and ideal Donnan model. Experimental results for Cl^- are denoted by ▲.

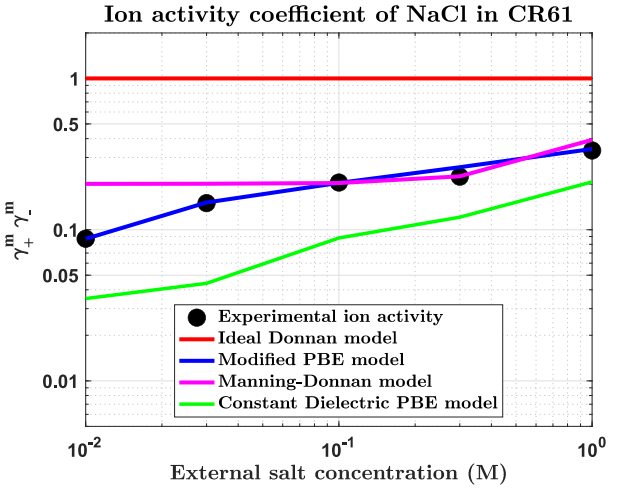

Figure 8. Comparison of ion activity coefficients from experimental data and estimated from the variable dielectric permittivity modified-PBE, constant dielectric permittivity PBE, Manning–Donnan, and ideal Donnan models.

"limiting law" for polyelectrolytes. Mathematically, eq 25 approaches a plateau of $(e\xi)^{-1}$ at low external salt concentration,[19] and hence the model is not sensitive to changes in external concentration at low values of external salt concentration. In the original article in which the Manning–Donnan model was first presented, this deviation is related to the breakdown of one or more of the assumptions used in the Manning model.[18]

In our modified-PBE model, the immobile counterions in the Stern layer are fundamentally similar to Manning's "condensed ions". Figure 8 presents ion activity coefficients calculated with a constant dielectric permittivity, and the value is much lower than the experimental data. This is due to the overprediction of co-ion concentration, as shown in Figure 7. The ion activity coefficients calculated by the modified-PBE model fits the experimental data well at lower concentration better than the Manning–Donnan model. During this process of improving the prediction of ion activity coefficients we have included two fitting parameters in the modified-PBE model, whereas the Manning–Donnan model has no adjustable parameters.

The modified PBE model was further used to predict equilibrium uptakes of NaCl, LiCl, and KCl in CR61 from work by Galizia et al.[54] The x_s (Stern layer thickness) values were set to 2 Å for KCl, 3 Å for NaCl, and 4 Å for LiCl, based on Stokes radii. The charge density used in the Stern and diffuse layers for NaCl, LiCl, and KCl are shown in Figure S5 in the Supporting Information. The ion activity coefficients calculated by the modified-PBE are plotted against the measured ion activity coefficients in the parity plot in Figure 9. The difference in sorption is due to the fact that different

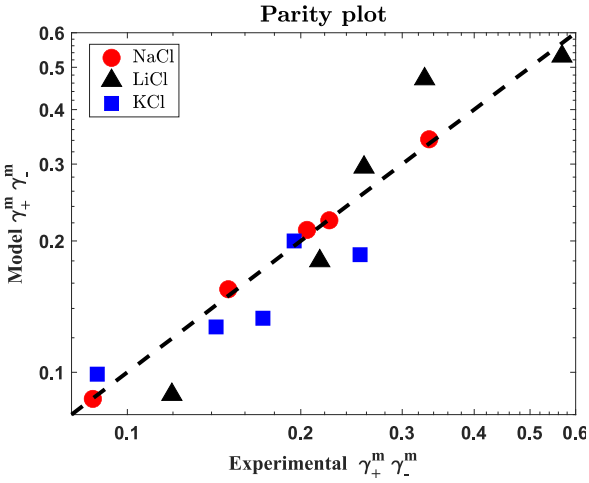

Figure 9. Parity plot between the modeled ion activity coefficients using the modified-PBE model and experimental ion activity coefficients. Model performance is plotted against the experimental values for NaCl (red ●), LiCl (black ▲), and KCl (blue ■).

counterions have different hydration energies. The hydration energies for different counterions display the following trend: La^{3+}> Mg^{2+}> Ca^{2+} > Li^+ > Na^+ > K^+ > Cs^+.[59] This effect is taken into account by the hydration constants in the modified-PBE model, and hence our model is quite consistent with the experimental results. On the other hand, Manning–Donnan

https://doi.org/10.1021/acsomega.2c02258
ACS Omega 2022, 7, 30823−30834

model predictions of equilibrium uptake are not sensitive to the counterion type.

CONCLUSIONS

The concentration and ion activity coefficients in ion exchange membranes are modeled using a general electrical double-layer theory that includes changes in the hydration free energy of ions. These ion hydration effects in the polymer matrix of highly charged polymers arise from changes in dielectric permittivity of the solvent induced by large electric fields. When the dielectric saturation effect is considered, the model does a good job describing the ion concentration and ion activity coefficients. Model predictions are compared to experimental data and to existing models of ion activity. All parameters in this general model have a physical basis and can be related to key experimentally measured properties. In this article we have used values for these parameters based on similar previous modeling efforts to describe charge distribution in charged membranes. The following conclusions are drawn from this work.

- Accounting for dielectric saturation allows us to quantitatively match the ion activity coefficients in highly charged membranes, particularly at lower external salt concentrations.
- The effect of dielectric saturation can be quantified by accounting for variable dielectric permittivity and the hydration free energy of ions in the PB equation. When these effects are taken into account in our model, the ion activity coefficients and concentrations are shown to accurately match experimental data.
- Accounting for dielectric saturation effects results in ion concentration profiles that show nonmonotonic trends and are quite different from those predicted by classical Gouy−Chapman double-layer theory.

As future efforts focus on the experimental determination of the values of membrane charge density, free volume thickness and Stern layer thickness will make it possible to improve the robustness of the modeling approach described in this work.

ASSOCIATED CONTENT

Supporting Information

The Supporting Information is available free of charge at https://pubs.acs.org/doi/10.1021/acsomega.2c02258.

Illustration of symmetry conditions, additional results, and charge density used in this study (PDF)

AUTHOR INFORMATION

Corresponding Author

Akhilesh Paspureddi − *The University of Texas at Austin, Department of Chemical Engineering, Austin, Texas 78712, United States;* orcid.org/0000-0002-3568-9034; Phone: 737-618-0074; Email: akhil_p@utexas.edu

Authors

Mukul M. Sharma − *The University of Texas at Austin, Department of Chemical Engineering, Austin, Texas 78712, United States; The University of Texas at Austin, Department of Petroleum and Geosystems Engineering, Austin, Texas 78712, United States*

Lynn E. Katz − *The University of Texas at Austin, Department of Civil, Architectural, and Environmental Engineering, Austin, Texas 78712, United States*

Complete contact information is available at: https://pubs.acs.org/10.1021/acsomega.2c02258

Notes

The authors declare no competing financial interest.

ACKNOWLEDGMENTS

This work was supported as part of the Center for Materials for Water and Energy Systems (M-WET), an Energy Frontier Research Center funded by the U.S. Department of Energy, Office of Science, Basic Energy Sciences under Award #DE-SC0019272.

NOMENCLATURE

symbol	definition
σ_0	surface charge density on the polymer with Stern layer
σ_d	charge density in the diffuse layer
σ_s	charge density in the Stern layer
ρ	volumetric charge density
ε	dielectric permittivity of the medium
ε_0	dielectric permittivity of free space
ε_b	dielectric permittivity of bulk water
$\varepsilon(r)$	dielectric permittivity of the medium at a radial distance r from the polymer
$\psi(r)$	electrical potential at a radial distance r from the polymer
ψ^m	electrical potential in the membrane
ψ^s	electrical potential in solution
ψ_m	electrical potential at the center of the free volume
ζ_{pot}	ζ potential
$E(r)$	electric field at a radial distance r from the polymer
$c_i^m(r)$	concentration of ith ion inside the membrane
c_i^b	concentration of ith ion in the bulk solution, same as C_S
$\overline{C}_i^m$	average concentration of ith ion in the membrane
C_S	concentration of external salt solution
ΔG_i	Free energy change of ith ion
H_i	hydration constant of ith ion, prefactor in the free energy of ith ion
z_i	valency of ith ion
x_s	Stern layer thickness
r	radial distance from the polymer
r_m	radial distance to the center line between two polymers
r_t	Total size of the EDL (Stern layer + diffuse layer + polymer radius)
r_s	Stern layer radius ($r_o + x_s$)
r_i	radius of ith ion
r_o	radius of polymer
$\overline{\mu}_i^m$	electrochemical potential in the membrane for ith ion
$\overline{\mu}_i^s$	electrochemical potential in solution for the ith ion
γ_i^j	activity coefficient of ith ion in the j phase
$\gamma_+^m\gamma_-^m$	ion activity coefficients of monovalent salt in the membrane
$\gamma_\pm^S$	mean ion activity in solution
ξ	Manning parameter
λ_B	Bjerrum length
b	distance between fixed charges
n_e	concentration of fixed charges
n_s	concentration of co-ions
n_c	concentration of counterions
η	refractive index of water
μ	dipole moment of water molecule

https://doi.org/10.1021/acsomega.2c02258
ACS Omega 2022, 7, 30823−30834

F	Faraday's constant
k	Boltzmann's constant
T	absolute temperature

REFERENCES

(1) Kamcev, J.; Freeman, B. D. Charged Polymer Membranes for Environmental/Energy Applications. *Annu. Rev. Chem. Biomol. Eng.* **2016**, *7* (1), 111−133.

(2) Kamcev, J. *Ion Sorption and Transport in Ion Exchange Membranes: Importance of Counter-Ion Condensation*, The University of Texas at Austin, 2016. DOI: 10.15781/T2959CD1D.

(3) Strathmann, H. *Ion-Exchange Membrane Separation Processes*; Elsevier: 2004; Vol. *9*.

(4) Xu, T.; Huang, C. Electrodialysis-Based Separation Technologies: A Critical Review. *AIChE J.* **2008**, *54* (12), 3147−3159.

(5) Landsman, M. R.; Sujanani, R.; Brodfuehrer, S. H.; Cooper, C. M.; Darr, A. G.; Davis, R. J.; Kim, K.; Kum, S.; Nalley, L. K.; Nomaan, S. M.; Oden, C. P.; Paspureddi, A.; Reimund, K. K.; Rowles, L. S.; Yeo, S.; Lawler, D. F.; Freeman, B. D.; Katz, L. E. Water Treatment: Are Membranes the Panacea? *Annu. Rev. Chem. Biomol. Eng.* **2020**, *11*, 559−585.

(6) Ticianelli, E. A.; Derouin, C. R.; Redondo, A.; Srinivasan, S. Methods to Advance Technology of Proton Exchange Membrane Fuel Cells. *J. Electrochem. Soc.* **1988**, *135* (9), 2209−2214.

(7) Geise, G. M.; Paul, D. R.; Freeman, B. D. Fundamental Water and Salt Transport Properties of Polymeric Materials. *Prog. Polym. Sci.* **2014**, *39* (1), 1−42.

(8) Nagasawa, M.; Izumi, M.; Kagawa, I. Colligative Properties of Polyelectrolyte Solutions. V. Activity Coefficients of Counter- and By-Ions. *J. Polym. Sci.* **1959**, *37* (132), 375−383.

(9) Fisher, M. E.; Levin, Y. Criticality in Ionic Fluids: Debye-Hückel Theory, Bjerrum, and Beyond. *Phys. Rev. Lett.* **1993**, *71* (23), 3826−3829.

(10) Robinson, R. A.; Stokes, R. H.. *Electrolyte Solutions*; Courier Corporation: 2002.

(11) Chang, K.; Geise, G. M. Dielectric Permittivity Properties of Hydrated Polymers: Measurement and Connection to Ion Transport Properties. *Ind. Eng. Chem. Res.* **2020**, *59* (12), 5205−5217.

(12) Paddison, S. J.; Reagor, D. W.; Zawodzinski, T. A. High Frequency Dielectric Studies of Hydrated Nafion. *J. Electroanal. Chem.* **1998**, *459* (1), 91−97.

(13) Ostwald, W. Studien Uber Die Bildung and Umwandlung Fester Korper. *Z.Phys. Chem.* **1897**, *22289* (1). DOI: 10.1515/zpch-1897-2233.

(14) Donnan, F. G. The Theory of Membrane Equilibria. *Chem. Rev.* **1924**, *1* (1), 73−90.

(15) Tamamushi, R.; Goto, S. Determination of Ion Activity Coefficients from the Measurement of Membrane Concentration Potentials - Activity Behavior of Alkali-Metal Cations in Aqueous Solution at 25 C. *Bull. Chem. Soc. Jpn.* **1970**, *43*, 3420−3424.

(16) Boyd, G. E.; Bunzl, K. The Donnan Equilibrium in Cross-Linked Polystyrene Cation and Anion Exchangers. *J. Am. Chem. Soc.* **1967**, *89* (8), 1776−1780.

(17) Freeman, D. H.; Patel, V. C.; Buchanan, T. M. Electrolyte Uptake Equilibria with Low Cross-Linked Ion-Exchange Resins. *J. Phys. Chem.* **1965**, *69* (5), 1477−1481.

(18) Kamcev, J.; Paul, D. R.; Freeman, B. D. Ion Activity Coefficients in Ion Exchange Polymers: Applicability of Manning's Counterion Condensation Theory. *Macromolecules* **2015**, *48* (21), 8011−8024.

(19) Manning, G. S. Limiting Laws and Counterion Condensation in Polyelectrolyte Solutions II. Self-Diffusion of the Small Ions. *J. Chem. Phys.* **1969**, *51* (3), 934−938.

(20) Kitto, D.; Kamcev, J. Manning Condensation in Ion Exchange Membranes: A Review on Ion Partitioning and Diffusion Models. *J. Polym. Sci.* **2022**, *2021*, 1−45.

(21) Oldham, K. B. A Gouy-Chapman-Stern Model of the Double Layer at a (Metal)/(Ionic Liquid) Interface. *J. Electroanal. Chem.* **2008**, *613* (2), 131−138.

(22) Loosley-Millman, M. E.; Rand, R. P.; Parsegian, V. A. Effects of Monovalent Ion Binding and Screening on Measured Electrostatic Forces between Charged Phospholipid Bilayers. *Biophys. J.* **1982**, *40* (3), 221−232.

(23) Biesheuvel, P. M.; Van Der Veen, M.; Norde, W. A Modified Poisson-Boltzmann Model Including Charge Regulation for the Adsorption of Ionizable Polyelectrolytes to Charged Interfaces, Applied to Lysozyme Adsorption on Silica. *J. Phys. Chem. B* **2005**, *109* (9), 4172−4180.

(24) Zhulina, E. B.; Borisov, O. V. Poisson-Boltzmann Theory of PH-Sensitive (Annealing) Polyelectrolyte Brush. *Langmuir* **2011**, *27* (17), 10615−10633.

(25) Ben-Yaakov, D.; Andelman, D.; Podgornik, R.; Harries, D. Ion-Specific Hydration Effects: Extending the Poisson-Boltzmann Theory. *Curr. Opin. Colloid Interface Sci.* **2011**, *16* (6), 542−550.

(26) Tandon, R.; Pintauro, P. N. Divalent/Monovalent Cation Uptake Selectivity in a Nafion Cation-Exchange Membrane: Experimental and Modeling Studies. *J. Membr. Sci.* **1997**, *136* (1−2), 207−219.

(27) Bontha, J. R.; Pintauro, P. N. Prediction of Ion Solvatlon Free Energies in a Polarizable Dielectric Continuum. *J. Phys. Chem.* **1992**, *96* (19), 7778−7782.

(28) Bontha, J. R.; Pintauro, P. N. High Frequency Dielectric Studies of Hydrated Nafion. *J. Electroanal. Chem.* **1998**, *49* (23), 3835−3851.

(29) Lee, H. J.; Choi, J. H.; Cho, J.; Moon, S. H. Characterization of Anion Exchange Membranes Fouled with Humate during Electrodialysis. *J. Membr. Sci.* **2002**, *203* (1−2), 115−126.

(30) Brown, M. A.; Goel, A.; Abbas, Z. Effect of Electrolyte Concentration on the Stern Layer Thickness at a Charged Interface. *Angew. Chemie - Int. Ed.* **2016**, *55* (11), 3790−3794.

(31) Brown, M. A.; Bossa, G. V.; May, S. Emergence of a Stern Layer from the Incorporation of Hydration Interactions into the Gouy-Chapman Model of the Electrical Double Layer. *Langmuir* **2015**, *31* (42), 11477−11483.

(32) Chen, S. L.; Krishnan, L.; Srinivasan, S.; Benziger, J.; Bocarsly, A. B. Ion Exchange Resin/Polystyrene Sulfonate Composite Membranes for PEM Fuel Cells. *J. Membr. Sci.* **2004**, *243* (1−2), 327−333.

(33) Ohshima, H.; Ohki, S. Donnan Potential and Surface Potential of a Charged Membrane. *Biophys. J.* **1985**, *47* (5), 673−678.

(34) Nightingale, E. R. Phenomenological Theory of Ion Solvation. Effective Radii of Hydrated Ions. *J. Phys. Chem.* **1959**, *63* (9), 1381−1387.

(35) Brown, M. A.; Abbas, Z.; Kleibert, A.; Green, R. G.; Goel, A.; May, S.; Squires, T. M. Determination of Surface Potential and Electrical Double-Layer Structure at the Aqueous Electrolyte-Nanoparticle Interface. *Phys. Rev. X* **2016**, *6* (1), 1−12.

(36) Lakshminarayanaiah, N. Measurement of Membrane Potential and Estimation of Effective Fixed-Charge Density in Membranes. *J. Membr. Biol.* **1975**, *21* (1), 175−189.

(37) Basu, S.; Sharma, M. M. Effect of Dielectric Saturation on Disjoining Pressure in Thin Films of Aqueous Electrolytes. *J. Colloid Interface Sci.* **1994**, *165*, 355−366.

(38) Tamagawa, H.; Taya, M. A Theoretical Prediction of the Ions Distribution in an Amphoteric Polymer Gel. *Mater. Sci. Eng., A* **2000**, *285* (1−2), 314−325.

(39) Fixman, M. The Poisson-Boltzmann Equation and Its Application to Polyelectrolytes. *J. Chem. Phys.* **1979**, *70* (11), 4995−5005.

(40) Born, M. Über Die Beweglichkeit Der Elektrolytischen Ionen. *Zeitschrift für Phys.* **1920**, *1* (3), 221−249.

(41) Grahame, D. C. Effects of Dielectric Saturation upon the Diffuse Double Layer and the Free Energy of Hydration of Ions. *J. Chem. Phys.* **1950**, *18* (7), 903−909.

https://doi.org/10.1021/acsomega.2c02258
ACS Omega 2022, 7, 30823−30834

(42) Epsztein, R.; Shaulsky, E.; Qin, M.; Elimelech, M. Activation Behavior for Ion Permeation in Ion-Exchange Membranes: Role of Ion Dehydration in Selective Transport. *J. Membr. Sci.* **2019**, *580*, 316−326.
(43) Kaps, P.; Rentrop, P. Generalized Runge-Kutta Methods of Order Four with Stepsize Control for Stiff Ordinary Differential Equations. *Numer. Math.* **1979**, *33* (1), 55−68.
(44) Basu, S.; Sharma, M. Effect of Dielectric Saturation on Disjoining Pressure in Thin Films of Aqueous Electrolytes. *J. Colloid Interface Sci.* **1994**, *165*, 355−366.
(45) Guggenheim, E. The Conceptions of Electrical Potential Difference between Two Phases and the Individual Activities of Ions. *J. Phys. Chem.* **1927**, *336*, 842−849.
(46) Helfferich, F. G. *Ion Exchange*; Courier Corporation: 1995.
(47) Zemaitis, J. F., Jr., Clark, D. M., Rafal, M.; Scrivner, N. C. *Handbook of Aqueous Electrolyte Thermodynamics: Theory & Application*; Wiley: 2010.
(48) Pitzer, K. S. Thermodynamics of Electrolytes. I. Theoretical Basis and General Equations. *J. Phys. Chem.* **1973**, *77* (2), 268−277.
(49) Pitzer, K. S.; Mayorga, G. Thermodynamics of electrolytes. II. Activity and osmotic coefficients for strong electrolytes with one or both ions univalent. *J. Phys. Chem.* **1973**, *77*, 2300−2308.
(50) Basu, S.; Sharma, M. M. An Improved Space-Charge Model for Flow through Charged Microporous Membranes. *J. Membr. Sci.* **1997**, *124* (1), 77−91.
(51) Ataka, K. I.; Yotsuyanagi, T.; Osawa, M. Potential-Dependent Reorientation of Water Molecules at an Electrode/Electrolyte Interface Studied by Surface-Enhanced Infrared Absorption Spectroscopy. *J. Phys. Chem.* **1996**, *100* (25), 10664−10672.
(52) Booth, F. The Dielectric Constant of Water and the Saturation Effect. *J. Chem. Phys.* **1951**, *19* (4), 391−394.
(53) Debye, B. Y. P. Part I. Dielectric Constant. Energy Absorption in Dielectrics With Polar Molecules. *Trans. Faraday Soc.* **1934**, *30*, 679−684.
(54) Galizia, M.; Benedetti, F. M.; Paul, D. R.; Freeman, B. D. Monovalent and Divalent Ion Sorption in a Cation Exchange Membrane Based on Cross-Linked Poly (p-Styrene Sulfonate-Co-Divinylbenzene. *J. Membr. Sci.* **2017**, *535* (March), 132−142.
(55) Mauro, A. Space Charge Regions in Fixed Charge Membranes and the Associated Property of Capacitance. *Biophys. J.* **1962**, *2* (2), 179−198.
(56) Burns, D. B.; Zydney, A. L. Buffer Effects on the Zeta Potential of Ultrafiltration Membranes. *J. Membr. Sci.* **2000**, *172* (1−2), 39−48.
(57) Delville, A. Interactions between Ions and Polyelectrolytes. A Note on Determination of Ionic Activities, with Reference to a Modified Poisson-Boltzmann Treatment. *Biophys. Chem.* **1984**, *19* (2), 183−189.
(58) Kamcev, J.; Galizia, M.; Benedetti, F. M.; Jang, E. S.; Paul, D. R.; Freeman, B. D.; Manning, G. S. Partitioning of Mobile Ions between Ion Exchange Polymers and Aqueous Salt Solutions: Importance of Counter-Ion Condensation. *Phys. Chem. Chem. Phys.* **2016**, *18* (8), 6021−6031.
(59) Pashley, R. M. Hydration Forces between Mica Surfaces in Electrolyte Solutions. *Adv. Colloid Interface Sci.* **1982**, *16* (1), 57−62.

https://doi.org/10.1021/acsomega.2c02258
ACS Omega 2022, 7, 30823−30834